Received: 22 May 2018
DOI: 10.1002/mop.31509

WILEY

RESEARCH ARTICLE

28 GHz Taylor feed network for sidelobe level reduction in 5G phased array antennas

Timothy A. Hill | **James R. Kelly**

Institute for Communication Systems (5GIC), University of Surrey, Guildford, Surrey, United Kingdom

Correspondence
Timothy A. Hill, Institute for Communication Systems (5GIC), University of Surrey, Guildford, Surrey GU2 7XH, United Kingdom.
Email: t.hill@surrey.ac.uk

Funding information
UK Engineering and Physical Sciences Research Council (EPSRC); 5G Innovation Centre, University of Surrey.

Abstract

This paper presents a design procedure for a phased array feed network. The procedure is validated by designing and fabricating a set of 28 GHz 8-element beam steerable antennas. Within the feed, a Taylor n-bar amplitude taper is implemented using unequal power dividers. At boresight, the taper reduced the sidelobe level by 2.84 dB to −15.2 dB. Beam steering from 0° to 48° is achieved using meanders. An empirical formula for the meander widths is proposed, enabling independent control of amplitude and phase. Empirical formulae for the initial parameters of the unequal dividers are also proposed. The wide transmission lines in this feed network are compatible with low-cost PCB fabrication techniques.

KEYWORDS

amplitude taper, beam scanning, microstrip, millimeter wave, unequal dividers

1 | INTRODUCTION

Interference is a key problem for future 5G communication networks, especially as the user density increases. Millimeter wave beamforming antennas will need to direct power towards intended users, and minimize the power transmitted or received in other directions.[1]

A non-uniform amplitude taper can be applied to reduce the sidelobe level (SLL) of a phased array antenna. This is achieved at the expense of a slight increase in main lobe beamwidth (i.e., gain reduction). The Taylor n-bar distribution achieves an optimal trade-off between gain and SLL.[2]

Several reported designs have implemented an amplitude taper within a phased array feed network. In Ref. [3], a Taylor distribution, having an SLL of −17 dB, was implemented within a 10-element array. This was achieved by adjusting the widths of transmission lines used to implement quarter wave transformers. However, a series feeding arrangement was used, which limits the beam steering range.[4] Alternatively, Ref. [5] used Y-junction dividers, together with an electromagnetic bandgap (EBG) structure to suppress surface waves. The antenna exhibited a very wide frequency operating bandwidth from 55 to 65 GHz along with an SLL of −13 dB across the whole bandwidth. However, in narrowband designs, the use of an EBG may be an unnecessarily complex way to address this issue, as surface waves can instead be suppressed by the use of a thin substrate.[1]

Technologies other than microstrip reduce unwanted radiation from the feed, to achieve a low SLL. They can also reduce the insertion loss, but are more costly and complex to manufacture. In Ref. [6], subarrays of 2 × 2 elements with an SLL of −13 dB were combined into a 16 × 16 element array with an SLL of −25 dB. Within the waveguide feed, the septum offsets and port widths of the unequal dividers were adjusted to achieve a 2D amplitude taper. Ref. [7] presented a substrate integrated coaxial line (SICL) feed achieving an x-direction and y-direction SLL of −19.6 dB and −18.0 dB, respectively. A Dolph-Chebyshev taper was produced by adjusting the radial dimensions of each blind via.

For electronically controlled beam shaping, an amplitude taper can be implemented using variable gain amplifiers or attenuators.[8]

In this paper, to increase the efficiency, we realize a fixed taper using power dividers. High power division ratios are required within the feed network. Using conventional unequal dividers, this necessitates narrow, high impedance lines, which are difficult to fabricate using standard printed circuit board (PCB) etching techniques. To address this problem, Ref. [9] proposed an unequal power divider which replaces these narrow lines with wider stubs, making them easier to manufacture.

For the first time, we propose a design procedure for a feed network based on this unequal divider. The procedure has several advantages.

First, to satisfy manufacture constraints, we propose formulae for the initial parameters (degrees-of-freedom) of the unequal dividers. This enables independent control over the widths of the lines in the unequal dividers. Second, to steer the main beam, meanders are used to produce fixed phase shifts. We propose a formula for the width of a meander line required to achieve a 50 Ω impedance. Correctly choosing this width, which varies as a function of meander length, minimizes any amplitude variation caused by beam steering. This enables independent control over the amplitude and phase at each element. Third, we take advantage of the convenience and low cost of microstrip while minimizing the adverse effect of the feed on the radiation pattern. The feed was implemented on a single layer of microstrip, without vias.

The procedure is also suitable for other planar technologies, such as stripline, coplanar waveguide (CPW) or substrate-integrated waveguide (SIW). Feed networks designed using the proposed procedure could find applications in mobile handsets or base stations.

2 | DESIGN PROCEDURE

This section of the paper describes the feed network design. The feed was connected to a phased array antenna for validation purposes. Starting from a target SLL, we determine the desired amplitudes and power split ratios, as well as the physical dimensions of the unequal dividers. Next, from the desired beam directions, we calculate the progressive phase shifts to be applied to each array element, and the corresponding meander dimensions.

2.1 | Step 1: design amplitude taper

The proposed feed network topology can be used to realize any desired amplitude distribution (for which voltage split ratios $K_i > 0.3$). For comparison, two different distributions were realized: (1) a uniform and (2) a Taylor n-bar distribution, given by the well-known expression[2]:

$$g(p) = 1 + 2\sum_{n=1}^{\overline{n}-1} F(n,A,\overline{n})\cos(n\pi p), \tag{1}$$

where $g(p)$ is the amplitude taper, $P = 2/L\ x$ is the aperture variable, $F(n, A, \overline{n})$ is a function used to produce array factor zeros of varying angular spacing, A is the SLL parameter, and $\overline{n}$ is the SLL roll-off parameter.

To obtain the amplitudes a_i of the signals at each array element, we express this as:

$$a_i = 1 + 2\sum_{n=1}^{\overline{n}-1} F(n,A,\overline{n})\cos\left(n\pi d\left(i - \frac{N+1}{2}\right)\right), \tag{2}$$

where N is the number of array elements, $i = 1, 2, 3 \ldots N$, and d is the spacing between elements.

For a typical 5G base station application, a beamwidth of 20° is required. This provides an adequate link range (cell radius), while limiting the effect of pointing errors on beam alignment. An SLL below −10 dB is required to suppress interference. A value of $\overline{n} = 20$ was chosen to achieve a suitable compromise between gain and SLL. Given that SLL is known to increase with steering angle,[2] a value of SLL = −20 dB was chosen for boresight. The Matlab command taylorwin(8,20,-40) was used to calculate the distribution, where $N = 8$ elements, and −40 dB is the SLL expressed as a voltage ratio.

2.2 | Step 2: determine voltage/power split ratios

The feed network consists of several junctions, each containing a power divider (Figure 1). Each junction is numbered for ease of reference. The desired amplitudes, calculated in step 1, are realized by appropriately setting the voltage split ratio (K_i) and power split ratio (J_i) at each junction. Power dividers (shown in Figure 2) are then designed to implement these ratios.

$$K_i = \frac{V_{i3}}{V_{i2}} = \sqrt{J_i}, \tag{3}$$

$$J_i = \frac{P_{i3}}{P_{i2}}, \tag{4}$$

$$J_1 = \frac{a_1 + a_2 + a_3 + a_4}{a_5 + a_6 + a_7 + a_8}, \tag{5a}$$

$$J_2 = \frac{a_1 + a_2}{a_3 + a_4}, \tag{5b}$$

$$J_3 = \frac{a_5 + a_6}{a_7 + a_8}, \tag{5c}$$

$$J_4 = \frac{a_1}{a_2}, \tag{5d}$$

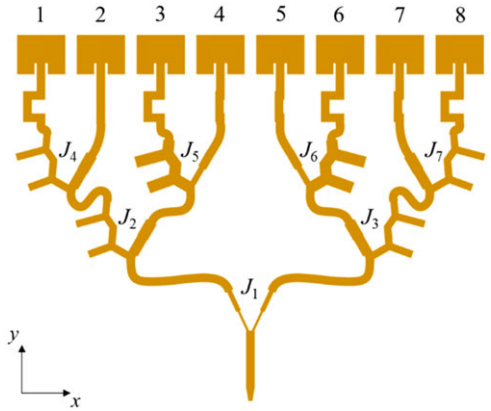

FIGURE 1 Proposed Taylor feed network (boresight). The transmission lines within the unequal dividers are much wider than for conventional unequal dividers [Color figure can be viewed at wileyonlinelibrary.com]

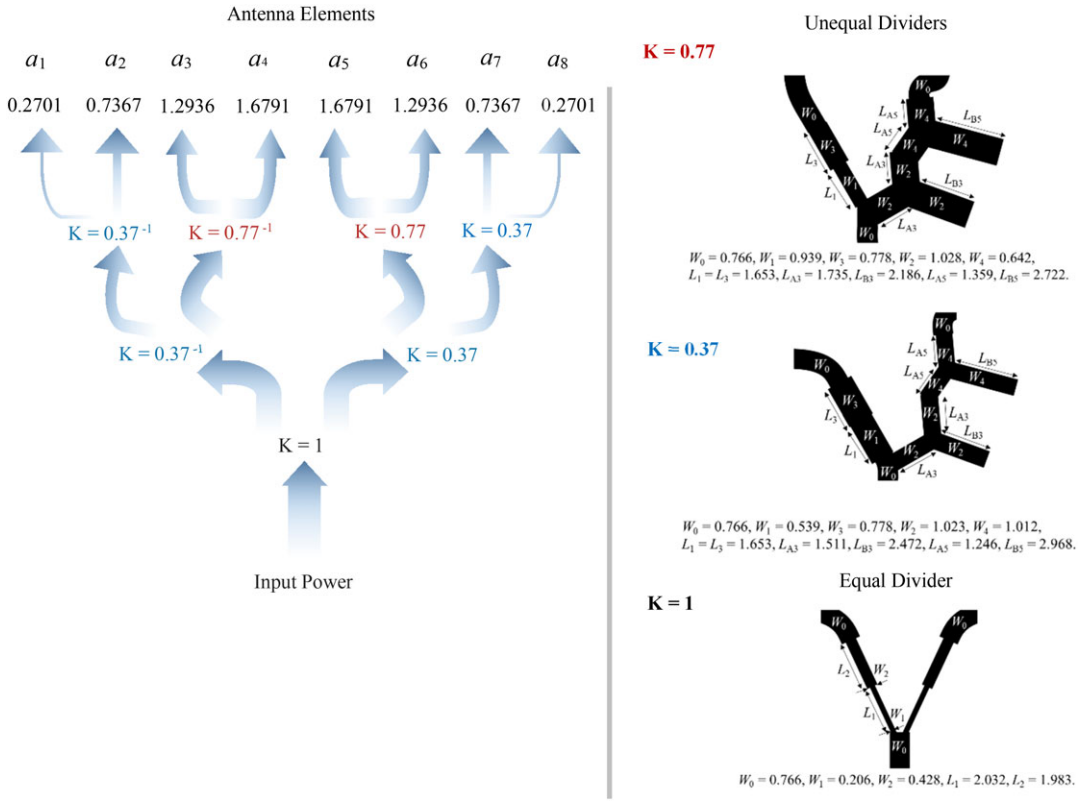

FIGURE 2 Voltage split ratios and unequal dividers within the feed network, to achieve the desired amplitudes. All physical dimensions are in mm. Port 2 of each divider is on the left, port 3 is on the right [Color figure can be viewed at wileyonlinelibrary.com]

$$J_5 = \frac{a_3}{a_4}, \tag{5e}$$

$$J_6 = \frac{a_5}{a_6}, \tag{5f}$$

$$J_7 = \frac{a_7}{a_8}, \tag{5g}$$

where V_2, V_3, P_2, and P_3 are the voltage and power levels at the respective output ports of each divider, and amplitudes a_i were defined in Equation 2.

2.3 | Step 3: design power dividers

At junction 1 of the Taylor feed, the power is split equally ($K_1 = 1$). This is implemented by a Wilkinson divider.[10] This equal divider was also used for all junctions within the uniform feed network.

For the unequal dividers, $K < 1$ is achieved by partial cancellation of incident and reflected currents in the stubs. To obtain values $K > 1$, the dividers were mirrored to give a voltage split $1/K$.

For ease of manufacture, we aim to meet the following constraints:

- Line width must be between 0.2 mm and 1.1 mm. This enables convenient fabrication and prevents the lines from overlapping at the divider junctions, avoiding impedance mismatch.
- Line length must be less than 4.25 mm. This enables the divider stubs to fit onto the PCB.

For example, if $K = 0.37$, a conventional unequal divider would require a line of width 12.4 μm. The divider from Ref. [9] achieves the same ratio using widths greater than 0.5 mm, which are much easier to fabricate.

Building on the method in Ref. [9] we propose empirical formulae for the values of the initial parameters of the unequal dividers: C, θ_{A3} and θ_{A5}. These parameters give us several degrees-of-freedom to meet the above constraints.

$$C \approx \frac{50}{K^{1.6}}, \text{valid for } 0 < K < 1, \tag{6}$$

$$\theta_{A3} \approx \frac{\pi}{4} + 0.69\sqrt[3]{1-K}, \text{valid for } 0.3 < K < 1, \tag{7a}$$

$$\theta_{A5} \approx \frac{\pi}{4} + 0.36\sqrt[3]{1-K}, \text{valid for } 0 < K < 1, \tag{7b}$$

where C is the arbitrary reference impedance in Ω, θ_{A3} and θ_{A5} are electrical lengths of transmission lines in radians. These formulae are valid only for the given frequency and substrate properties.

For each transmission line section, the required impedance and electrical length were determined using the procedure given in Ref. [9] We propose a modification to this

procedure, resulting in Equation 8, which makes the negative stub lengths positive and thus realizable using conventional transmission line technology.

$$\theta_{B3} = \begin{cases} tan^{-1}(2\cot(2\theta_{A3})) & \theta_{A3} > 0 \\ tan^{-1}(2\cot(2\theta_{A3})) + 2\pi & \theta_{A3} \le 0, \end{cases} \quad (8)$$

where θ_{B3} is a stub electrical length in radians. Equation 8 can also be used to calculate θ_{B5} from θ_{A5}. Note that θ_{A3}, θ_{B3}, θ_{A5}, and θ_{B5} correspond to physical lengths L_{A3}, L_{B3}, L_{A5}, and L_{B5}.

The corresponding physical lengths and widths were synthesized in microstrip technology using standard equations from Ref. [10] and are shown in Figure 2. The chosen substrate was Rogers RT duroid 5880 ($\varepsilon_r = 2.2$, tan $\delta = 0.0009$ at 10 GHz) of thickness $h = 0.254$ mm, with copper of thickness 0.017 mm on both sides. The feed was connected to an 8-element array of microstrip patches with half-wavelength spacing.

2.4 | Step 4: determine required phase shifts

To steer the main beam of a phased array to an angle θ_0, a progressive phase shift β, given by Equation 9, must be applied between consecutive elements.[3] Table 1 provides the progressive phase shifts used, along with the associated beam directions.

$$\beta = -kdsin(\theta_0), \quad (9)$$

$$\Delta\varphi_i = \beta(i-1), \quad (10)$$

where $k = 2\pi/\lambda_0$, $d = \lambda_0/2$, and $\Delta\varphi_i$ is the phase shift at each element i relative to the input port. $\lambda_0 = 10.71$ mm is the free-space wavelength at the center frequency, $f_0 = 28$ GHz.

In a practical implementation of the feed network, dynamic beam steering could be achieved using phase shifter ICs. In this paper, for proof-of-concept, we fabricated several antenna PCBs (Figure 3). Each antenna has a different, fixed main beam direction. The consecutive phase shifts were realized using meandered sections of transmission line. We refer to these as beam steering meanders.

TABLE 1 Steered Taylor PCBs: phase shifts, beam directions, and meander widths and lengths in mm

β (°)	0	36	72	108	144
θ_0 (°)	0	−11.5	−23.6	−36.9	−53.1
W_{m1}, W_{m5}	0.766	0.766	0.766	0.766	0.766
W_{m2}, W_{m6}	0.766	0.7002	0.6345	0.5687	0.5030
W_{m3}, W_{m7}	0.766	0.6345	0.5030	0.371	0.5
W_{m4}, W_{m8}	0.766	0.5687	0.3175	0.24	0.5
W_{mright}	0.766	0.5030	0.24	0.24	0.24
L_{m1}, L_{m5}	0	0	0	0	0
L_{m2}, L_{m6}	0	0.794	1.588	2.382	3.176
L_{m3}, L_{m7}	0	1.588	3.176	4.764	6.352
L_{m4}, L_{m8}	0	2.382	4.764	7.146	9.528
L_{mright}	0	3.176	6.352	9.528	9.528

2.5 | Step 5: implement phase shifts

The meander length L_{mi} for element i is proportional to its electrical length (phase delay $\Delta\varphi_i$), see Equation 11.[10] To minimize feed radiation, it was necessary to keep the meander horizontal (i.e., x-axis) extent $L_{mi}/5$ below $\lambda_0/2$. Hence, their lengths were shared between a phase shift of 4β at the right arm of the first divider ($L_{m\ \mathrm{right}}$), and remaining phase shifts of [0, β, 2β, 3β, 0, β, 2β, 3β] at the steering meanders.

$$L_{mi} = \frac{\Delta\varphi_i}{2\pi}\lambda_g = \frac{\Delta\varphi_i}{2\pi}\frac{\lambda_0}{\sqrt{\varepsilon_{reff}}}, \quad (11)$$

where the effective relative permittivity ε_{reff} is calculated for each line width, as in Ref. [10]

Note that altering the length of the meandered section, to realize the desired phase shift, also alters the characteristic impedance of the transmission line. This occurs due to coupling between adjacent bends within the meander. In order to maintain a 50 Ω impedance, it is necessary to reduce the meander width W_{mi}. We obtained Equation 12 by fitting a piecewise straight line to impedances simulated for different meander lengths. It is valid only for the given frequency and substrate properties. This adjustment ensures that the meanders do not affect the amplitude distribution. The meander parameters are shown in Figure 3. Note that this formula is only accurate for $\Delta\varphi_i^\circ < 216°$. For longer meanders, it is recommended to fine-tune their widths via a parametric study.

$$W_{mi} \approx \begin{cases} 0.766 - \dfrac{\Delta\varphi_i^\circ}{547.5} & \Delta\varphi_i^\circ < 216^\circ \\ 0.371 & \Delta\varphi_i^\circ \ge 216^\circ. \end{cases} \quad (12)$$

In addition to the beam steering meanders, phase correction meanders were required. The absence of isolation resistors introduced a 35° phase error between the signals at the output ports of the divider. This error was compensated by additional line length (meanders) at the output ports of the feed. Their lengths, in the x-direction, are provided in Table 2. The width of all correction meanders is 0.766 mm (the same as a 50 Ω line). In the Taylor boresight ($\beta = 0°$) PCB, this phase correction ensured that the patches all radiated approximately in phase.

2.6 | Step 6: implement the connecting feed lines

Here, we aim to minimize the SLL of the phased array antenna, and maximize the feed network efficiency. This requires minimizing the level of radiation from the feed network, and a good impedance matching throughout the feed.

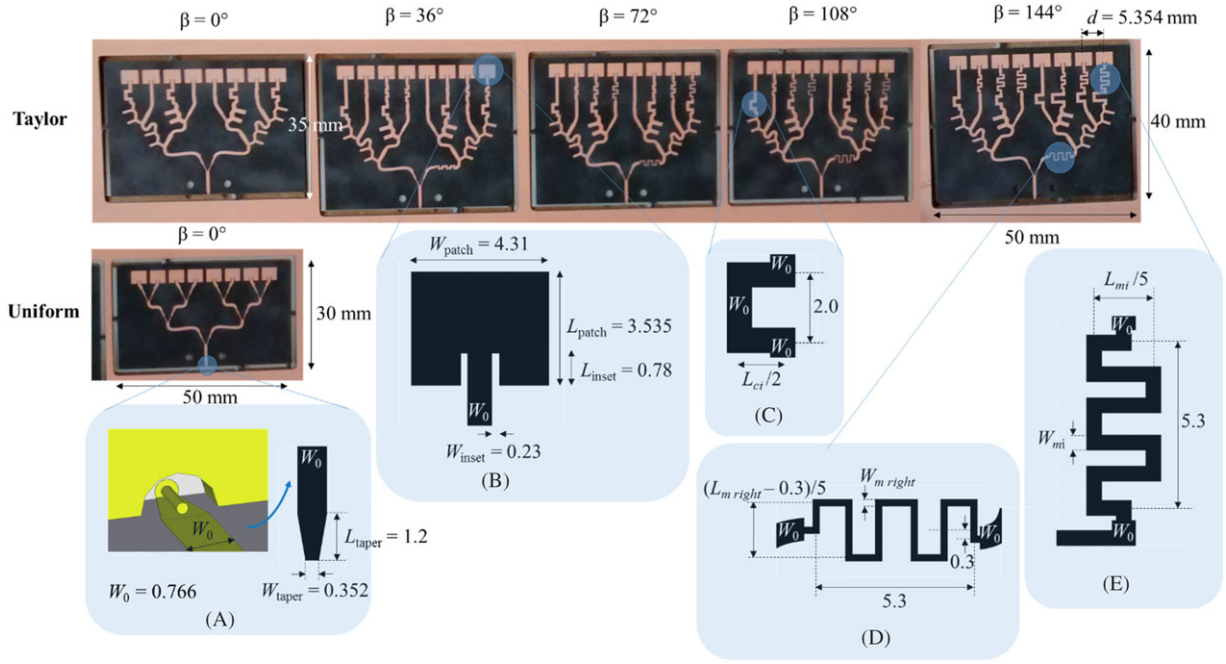

FIGURE 3 Photograph of the fabricated PCBs, with physical dimensions in mm. Inset: (A) tapered transition. This introduces inductance to compensate for the capacitance of the 2.92 mm connector pin. (B) Patch element. Its dimensions were calculated as in Ref.,[11] and W_{inset} was obtained by a parametric study. (C) Phase correction meander. (D) Right arm meander. (E) Beam steering meander [Color figure can be viewed at wileyonlinelibrary.com]

To achieve these, we recommend to:

- Keep the feed lines as short as possible, and avoid sharp bends.
- Ensure that the ends of the lines are parallel and aligned at their centers.
- Maintain a minimum separation of 0.68 mm between any stub and adjacent line, and a minimum bend radius of 0.65 mm.

3 | RESULTS

This section of the paper presents simulation and measurement results for a feed network designed using the procedure outlined in Section 2. The antenna PCBs were simulated in CST Microwave Studio 2016. The scatting parameters and radiation pattern were measured using a Rohde and Schwarz ZVA67 network analyzer, calibrated using the Open-Short-Match (OSM) procedure.

TABLE 2 Phase correction meander lengths in mm. L_{ci} corresponds to antenna element i

β (°)	0, 36, 72, 108	144
L_{c1}	2.437	2.437
L_{c2}	0	0
L_{c3}	2.274	2.274
L_{c4}	0.1654	0.1654
L_{c5}	0.2219	3.398
L_{c6}	2.635	5.811
L_{c7}	0.3079	3.484
L_{c8}	2.635	5.811

Figure 4 shows the simulated frequency variation in the scattering parameters of the Taylor feed. Port 1 is the input port, and ports 2-9 are the output ports connected to elements 1-8, respectively. In Figure 4A, $|S_{i1}|$ represents the simulated voltage splits from the input port to each element. The sum $\sum_{i=2}^{9} |S_{i1}|^2 = -0.66$ dB, which is equivalent to an efficiency of 85.9% at the center frequency. This indicates that the feed is low-loss.[10] The $|S_{11}| < -20$ dB bandwidth of the feed is 1.15 GHz, from 27.5 GHz to 28.65 GHz. Acceptable flatness of the voltage splits is observed across this bandwidth.

Figure 4B shows the frequency variation of the phase at the output ports of the feed network. For elements 3-6, which have the most power, the group delay varies by less than 9.4% across the operating bandwidth, indicating that

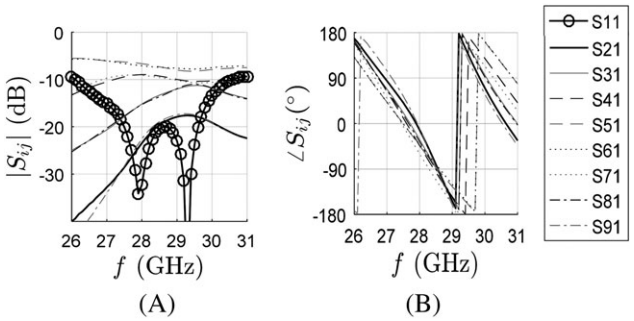

FIGURE 4 Taylor boresight feed network scattering parameter variation with frequency for all feed ports. (A) S parameter magnitudes. (B) S parameter phases, after correction

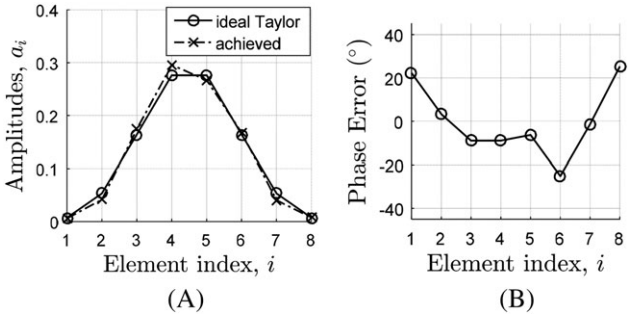

FIGURE 5 Achieved excitation at the feed output ports at 28 GHz. (A) Simulated and ideal Taylor amplitudes. (B) Phase error at the output of the feed, after correction

beam squint (and hence pointing loss) is kept within acceptable limits. This illustrates the validity and accuracy of our proposed design procedure.

Figure 5 shows the desired and achieved amplitude and phase distributions, associated with the Taylor boresight feed network at 28 GHz. Both the achieved and ideal amplitudes are normalized to the same total power value. The maximum amplitude error is 10% of the input power, and the maximum phase error between elements after correction is 25.3°. This phase error occurs for elements 1 and 8, which have the least amplitudes. As shown in Figure 6, these errors cause the SLL of the array factor to increase by around 8 dB. However, in the final radiation pattern, this effect will be reduced, due to pattern multiplication with the element factor. The amplitude errors are caused by the implementation of the K_i values, and the phase errors are caused by uncorrected line lengths. This observed effect of errors on the SLL agrees with the discussion in Ref. [2]

Figure 7 shows the input reflection coefficient $|S_{11}|$ for PCBs associated with boresight and the maximum steering angle. Good agreement is observed between simulation and measurement. For each PCB, the bandwidth is determined

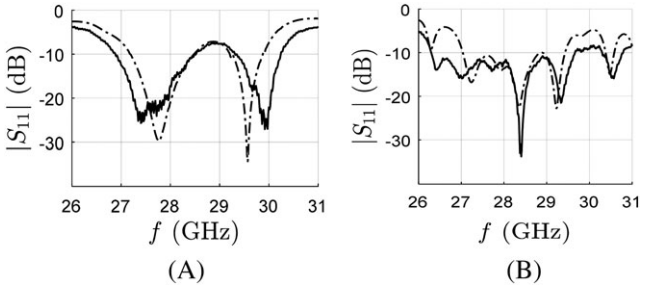

FIGURE 7 $|S_{11}|$, simulated (dash-dot line) and measured (solid line). (A) Boresight array (Taylor $\beta = 0°$). (B) Array steered to the maximum angle (Taylor $\beta = 144°$)

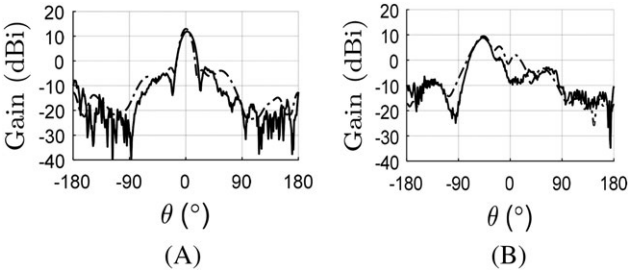

FIGURE 8 Radiation patterns, simulated (dash-dot line) and measured (solid line). (A) Boresight array (Taylor $\beta = 0°$). (B) Array steered to the maximum angle (Taylor $\beta = 144°$)

by the frequency domain poles (for which $|S_{11}| = 0$). These poles (resonances) are associated with the power dividers, meanders, and patches within the PCBs. A common −10 dB bandwidth of 0.95 GHz was achieved for all steering angles. This is considered sufficiently wide for 5G communications.

Figures 8 and 9 show the radiation patterns for the phased arrays shown in Figure 3. In Figure 8A, the measured SLL of −15.2 dB agrees well with the simulated value (−15.35 dB). The Taylor distribution reduced the SLL by 2.84 dB, compared to the radiation pattern for the

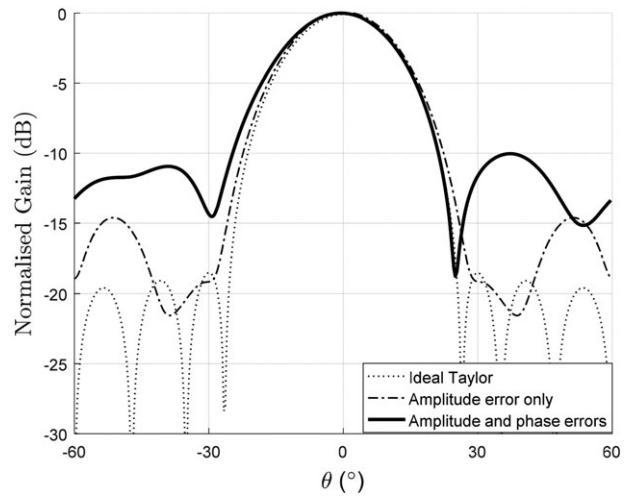

FIGURE 6 Simulated normalized array factor for an ideal Taylor distribution, and for the achieved amplitudes and phases

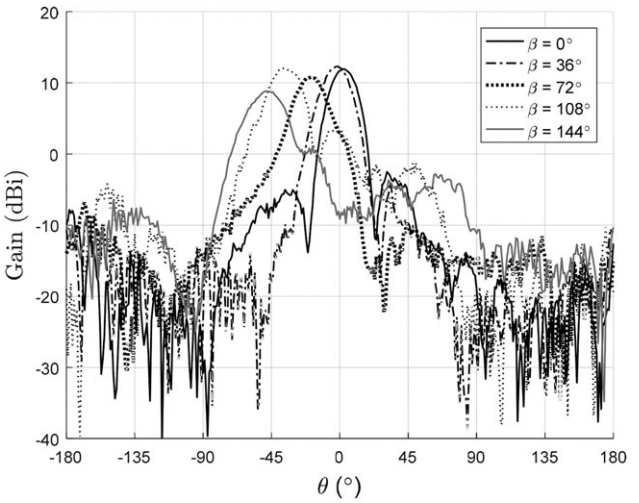

FIGURE 9 Measured radiation patterns for all steering angles. β is the progressive phase shift

uniform feed PCB (not shown). However, the main lobe gain decreased by 1.67 dB, to 11.5 dBi. Overall, this SLL reduction is beneficial and outweighs the gain reduction. Based on the simulated directivity of 13.6 dBi, the total efficiency of the antenna incorporating the Taylor boresight feed PCB is 66%. At the maximum steering angle of 48°, the scan loss is 2.9 dB, which is typical of a conventional phased array.

4 | CONCLUSION

In this paper, we presented a comprehensive design procedure for a feed network based on unequal power dividers. To validate the procedure, we designed and built a set of Taylor n-bar feed networks for a phased array antenna. A line width greater than 0.2 mm was maintained for all parts of the feed. The antenna arrays were fabricated at low cost, on a single layer of microstrip, with good agreement between measurement and simulation. An SLL below −15 dB was achieved at boresight. This SLL reduction will increase the signal-to-interference-and-noise ratio in 5G millimeter wave links, reducing interference. Future work will extend this method to realize arbitrary amplitude distributions and beam shapes.

ACKNOWLEDGMENTS

The authors would like to acknowledge Rogers Corporation, for providing substrate samples used to prototype this design. We would also like to acknowledge the support of EPSRC (EP/P008402/1) as well as the University of Surrey 5GIC (http://www.surrey.ac.uk/5gic).

ORCID


Timothy A. Hill https://orcid.org/0000-0001-9925-8498

REFERENCES

[1] Rappaport TS, Heath RW Jr, Daniels RC, Murdock JN. *Millimeter Wave Wireless Communications*. Upper Saddle River, NJ: Pearson Education; 2015:205-206, 472-474, 502-504.

[2] Hansen RC. *Phased Array Antennas*. Vol. 14. New York: Wiley Interscience; 1998:64-67, 465-467.

[3] Balanis CA. *Antenna Theory: Analysis and Design*. 2nd ed. New York: Wiley; 1997:267, 774, 869-870.

[4] Hamberger GF, Trummer S, Siart U, Eibert TF. A planar dual-polarized microstrip 1-D-beamforming antenna array for the 24-GHz band. *IEEE Trans Antennas Propag.* 2017;65(1):142-149.

[5] Briqech Z, Sebak AR, Denidni TA. Low-cost wideband mm-wave phased array using the piezoelectric transducer for 5G applications. *IEEE Trans Antennas Propag.* 2017;65(12): 6403-6412.

[6] Huang GL, Zhou SG, Chio TH, Hui HT, Yeo TS. A low profile and low sidelobe wideband slot antenna array fed by an amplitude-tapering waveguide feed-network. *IEEE Trans Antennas Propag.* 2015;63(1):419-423.

[7] Liu B, Zhao R, Ma Y, et al. A 45 degree linearly polarized slot array antenna with substrate integrated coaxial line technique. *IEEE Antennas Wireless Propagat Lett.* 2018;17(2):339-342.

[8] Evans E, Rock JC, Hudson T, Chaffin M, Wolfson B, Ashcom C, Lawrence D. Iteration of a MEMS-based, Ka-band, 16-element sub-array. In: Proceedings of the 2011 Aerospace Conference; 2011:1-13; Big Sky, MT.

[9] Yang T, Chen J, Xue Q. Novel approach to the design of unequal power divider with high-dividing ratio. *Microw Opt Technol Lett.* 2009;50(5):1240-1243.

[10] Pozar DM. *Microwave Engineering*. Vol 518. 3rd ed. , Hoboken, NJ: John Wiley & Sons, Inc; 2005:318-322.

[11] Huang K, Boyle Y. *Antennas: From Theory to Practice*. Chichester, UK: John Wiley & Sons Ltd; 2008:187-190.

How to cite this article: Hill TA, Kelly JR. 28 GHz Taylor feed network for sidelobe level reduction in 5G phased array antennas. *Microw Opt Technol Lett*. 2019;61:37–43. https://doi.org/10.1002/mop.31509